

Determining the Relationship between DNA Double Strand Breaks and Apoptosis: Implications for Cancer Therapy

A Major Qualifying Report:
submitted to the Faculty
of
Worcester Polytechnic Institute
on partial fulfillment of the requirements for the
Degree in Bachelors of Science
by

Jillian Brooks Earley

Date: April 21, 2023

Approved:

Professor José M. Argüello

Biochemistry

WPI Project Advisor

Sharon B. Cantor

Molecular, Cell, and Cancer Biology

UMass Chan Medical School

UMMS Project Advisor

This report represents the work of one or more WPI undergraduate students submitted to the faculty as evidence of completion of a degree requirement. WPI routinely publishes these reports on the web without editorial or peer review.

Abstract

This project sought to better understand a known effect of chemotherapies, the DNA Double Strand Break, and its effect on cell functioning. Increasing amounts of Double Strand Breaks (DSBs) were induced in Retinal Pigment Epithelial cells using CRISPR and confirmed via γ H2AX foci. The cellular response to these DSBs was explored through cell survival and apoptotic intensity. Apoptosis levels were indicated by quantifying nuclear abnormalities and active caspase-3/7 signals. Cells had decreased survival with increasing amounts of DSBs, and higher apoptotic levels in both nuclear morphology and caspase levels. Additionally, we analyzed cells deficient in hereditary breast and ovarian cancer gene, *BRCA1*, that are defective in DSB repair. Interestingly, BRCA1-deficient cell lines did not exhibit higher levels of cell demise nor apoptosis when compared to control lines. Likely buffering cell death in this context was Non-Homologous End Joining, a mechanism that functions in DSB repair and was found to be elevated in both cell lines following DSB inductions. Given that control and BRCA1-deficient cells respond similarly, loss of Homologous Recombination is not sufficient as a selective cancer therapy strategy following DSBs as induced here. Further exploration is needed to understand the complex cellular responses to DSB repair and the role of BRCA1 in DNA repair and cancer suppression.

Table of Contents

Title Page.....	1
Abstract.....	2
Table of Contents.....	3
Acknowledgements.....	4
Introduction.....	5
Methods.....	14
Results.....	19
Discussion.....	26
Bibliography.....	30
Supplementary Figures.....	33
Supplementary Figures 1: γ H2AX Triplicate Results.....	33
Supplementary Figures 2: Caspase-3/7 Assay Triplicate Results.....	34
Supplementary Figure 3: Nuclear Abnormalities Replicate.....	35

Acknowledgements

I am so thankful to those who have supported me throughout this research project. Thank you to Sharon Cantor, who welcomed me into her lab. You've set the standard for research practices and attentive reasoning though scientific questions. Thank you for this amazing opportunity.

Thank you to Jenna Whalen for being such an attentive mentor. Beyond demonstrating techniques in the lab, you showed me positivity and patience throughout research. Thank you to Ke, Nate, Silvia, and Mitch for creating such a great learning environment in the Cantor Lab.

Thank you to José Argüello, my WPI advisor, for your guidance throughout the project and in previous classes. I appreciate your feedback during meetings, and your advice for the future. I learned more than just science during this project experience; thank you for sharing your perspective.

Thank you to my family and friends for supporting me through this journey and my time at WPI. Thank you to my parents, and my POP, for inspiring my dedication and hard work. Thank you Gram, who is forever a comfort and with me always. To my siblings, for bringing me such joy. I appreciate all of your support so much.

Introduction

DNA Double Strand Breaks

As the name suggests, Double Strand Breaks (DSBs) are lesions that span both strands of the DNA double helix. Through the many factors and processes that cause DSBs, the resulting break can be a blunt or a staggered break, where the lesion is offset. External forces, such as ionizing radiation and many chemotherapies, are known to induce Double Strand Breaks¹. In addition, DSBs can occur without these external forces, as either spontaneous or cell mediated processes. For example, DSBs can occur spontaneously through replication fork stalling or collapse, but it also can be initiated during V(D)J recombination and meiotic recombination².

Effects of Double Strand Breaks

DSBs are considered the “most dangerous” type of DNA damage, threatening to a cell’s function as the cell cannot replicate or transcribe properly³. Normally, replication occurs at origins of replication, where a replication fork is formed as the strands of DNA separate, and that replication fork travels to allow the genome to be replicated. When the replisome encounters a Double Strand Break, large sections of genes could fail to be replicated. The break ends could also disassociate from one another, making proper recombination difficult⁴.

Replication stress occurs when the replisome encounters a barrier, causing the replication fork to stall, and if unable to be fixed, collapse⁵. Several types of barriers, one of which is DSBs, can impede fork progression, or the rapid proliferation of cells can cause replication stress through insufficient deoxynucleotide supply⁵. Replication fork stalling is a reversible pause during DNA replication. During fork stalling, ssDNA binding protein RPA protects the single strand DNA exposed in the fork⁶. The presence of ssDNA triggers the activation of the ATM-

and Rad3-Related Kinase (ATR), which organizes the replication stress response⁷. If the barrier impeding replication cannot be repaired, then the fork may collapse, which can also create a DSB⁷.

This replication stress can cause genomic instability, which is defined as the inability for parental cells to “accurately replicate the genome” and produce two correctly equipped daughter cells⁸. Genomic instability is thought to occur by an amplified degree of nucleotide mutations, small nucleotide repeats in the genome (microsatellite instability), or chromatin segregation that causes improper chromosome numbers⁹. Thus, genomic instability is characterized by mutations and the initiation of cancer⁸. There is a causal relationship between DNA DSBs and tumorigenesis, as the improper repair, or lack of repair, can cause chromosomal translocations¹⁰. This lends itself to the dysfunction or deletion of tumor suppressor genes, and it can amplify the expression of potentially oncogenic proteins³.

Double Strand Break Repair

Given that DSBs are detrimental to cell function, cells have developed robust responses to repair them. Homologous Recombination (HR) is a high-fidelity repair pathway during late S and G2 phases of the cell cycle, utilizing D-loop repair and homologous strand invasion to re-establish the duplex DNA strands¹¹. Non-Homologous End Joining (NHEJ) occurs predominantly in G1 phase, and reanneals the loose ends with little homology, often resulting in insertion/deletion of base pairs in the DNA^{12,13}. Other repair responses are utilized, such as Alternative End Joining (alt-EJ) and Single Strand Annealing (SSA).

Homologous Recombination processes involve the sensing the DSB, mediating end resection and Holliday junction formation, and the re-making of the DNA to fix the Double Strand Break. In the sensing of a DSB, the histone H2AX is phosphorylated by kinases such as ATR and ATM proteins, which are key players in DNA repair and stress pathways. The phosphorylation of the Ser139 position of H2AX at DSBs is an early player in the cell's DSB repair response, and it recruits and localizes proteins for subsequent steps of DNA repair^{14,15}. This phosphorylation is “one of the earliest events” following DNA damage of this sort, and thus it is a reliable and sensitive indicator of DSBs¹⁶.

Breast Cancer-Associated Gene 1 (BRCA1) is a key player in HR, present in multiple complexes that sense, mediate, and repair the Double Strand Break (Figure 1). The gene includes 22 exons, those 110 kilobases of DNA resulting in a 190 kilodalton protein¹⁷. This BRCA1 protein localizes to the nucleus, where it is functional. With different binding domains, the BRCA1 protein is able to form complexes with proteins involved in cell cycle suppression and HR¹⁸. BRCA proteins are key players in these DNA repair mechanisms. It is understood that the functional inactivation of the BRCA1 protein makes cells susceptible to tumorigenesis¹⁹. Specifically, mutations in the BRCT domain of the BRCA1 gene can cause dysfunction in DSB repair pathways, as the repair macro complexes cannot form without the bonding sites on BRCA1 proteins²⁰.

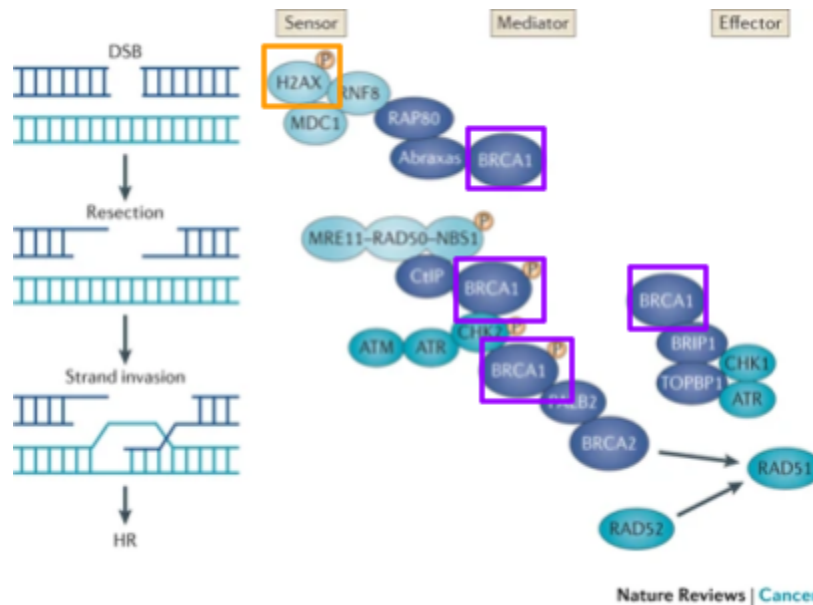


Figure 1: Roy, Chun, and Powell’s (2012) depiction of the molecular mechanisms involved in DNA Damage response for Homologous Recombination¹⁹. As shown, BRCA1 (purple boxes) is a common factor in the macro-complexes detecting Double Strand Breaks, recruiting proteins for damage repair procedures, and signaling for cell checkpoints. The phosphorylation of the H2AX histone (orange box) plays a key role in the detection of Double Strand Breaks.

Apoptosis

When DSBs are not repaired properly using cell mechanisms, the damage to DNA can initiate apoptosis, a form of programmed cell death (Figure 2). Unlike accidental cell death, such as necrosis, the regulated nature and process of apoptosis is “neat” and does not initiate the inflammatory response in tissues. Apoptosis is a large area of study due to its role in cell regulation in many circumstances: in embryonic development, regulation of potentially cancerous or virulent cells, and homeostasis, for example²¹. DNA damage is an “intrinsic” factor of apoptosis, and DNA damage thought to be accumulated through genotoxins and/or chemotherapy occurs through a p53-dependent pathway²¹.

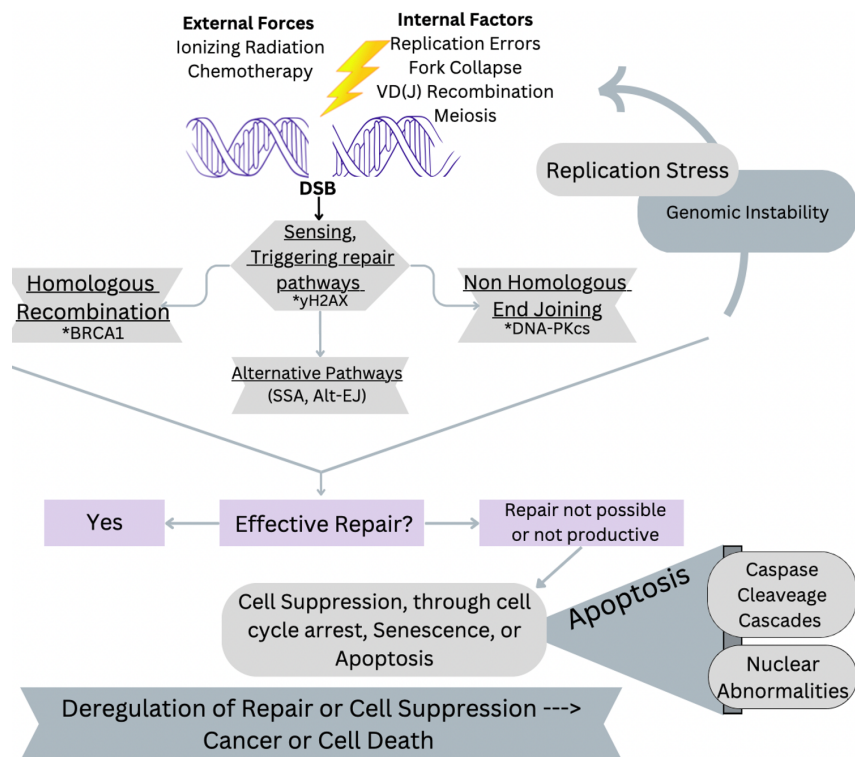


Figure 2: Constructed schematic for cell responses and pitfalls to Double Strand Breaks. Nonprogrammed damage, such as ionizing radiation, genotoxins, and replication errors, or programmed cell procedures can cause DSBs. After sensing the break, signal transduction triggers cell responses such as Homologous Recombination and Non-Homologous End Joining. Inability to repair DSBs can lead to replication stress, which is associated with fork collapse, and genomic instability. If repair is not effective, the cell induces apoptosis, arrests growth or cell division. Without regulated cell processes, cells die or develop into cancer cells.

Cysteine aspartate–specific proteases, also known as caspase proteins, are a large component of the apoptotic response. Two categories of caspase roles in apoptosis pathways are “initiator” and “effector” caspases. Effector caspases are known to do most of the proteolysis, or enzyme cleavage, that makes up the controlled apoptotic signaling pathway. To cleave proteins, the caspase family utilizes a cysteine residue in their active site to hydrolyze the peptide bond that follows an aspartate residue on the receiving enzyme. The precursor caspase often cleaves the next caspase in the apoptotic signaling pathway, changing it from its inactive, procaspase form into its active, cleaved, dimer conformation²².

Caspase-3, in its cleaved, active form, is a known executioner of apoptosis through the activation of DNA fragmentation and other cell-destructive mechanisms in the cytoskeleton^{23,24}. Because of its profound role in apoptosis, Caspase-3 is often targeted as a biomarker for apoptosis in cells. In addition, its fast conformation to its activated form once apoptosis pathways begin means that cleaved Caspase-3 can represent the timeline for apoptosis processes relatively accurately²⁶. Caspase-7 is also a known executioner of apoptosis and is understood to contribute to the apoptotic detachment of the cell²⁷.

Nuclear Abnormalities

“Nuclear abnormalities” are an observed phenotype that was defined as nuclear blebbing, multinucleation, catastrophic micronucleation, and polylobular nuclei. Fischer (2020) states that these nuclear abnormalities are a “key morphologic feature” of malignant cells²⁷. Nuclear morphology has been correlated with apoptosis²⁸. Though some studies have developed objective nuclear measurements such as form factor and nuclear circumference, another option when measuring abnormal nuclear morphology is to identify the ratio of nuclear abnormality instances in different experimental scenarios²⁸. Hollville and Martin (2016) identify fluorescent microscopy and Hoescht-stained nuclei as a “preferred method” for quantifying apoptosis²⁹. These phenotypes are different from the typical nuclear changes that occur during mitosis, which is the separation of replicated DNA into two nuclei. These nuclear abnormalities are clear signs of impending cell death, but their mechanisms are not fully understood³⁰.

BRCA-related Cancers

BRCA-deficient cancer cells are a type of cancer cell that lacks functional copies of the BRCA1 or BRCA2 genes. These genes are important for repairing DNA damage, and when they are not functioning properly, the cells are more prone to accumulating genetic mutations. Though a significant number of cancers arise through spontaneous mutation, 5-10% of breast cancer and 10-15% of ovarian cancers are hereditary. Mutations in the BRCA1 gene can disrupt the normal function of these proteins, leading to a deficiency in the ability to repair DNA damage. This can increase the risk of cancer, as the accumulation of genetic mutations can lead to the uncontrolled growth and division of cells. 80% of inherited breast and ovarian cancers are caused by a mutation in the BRCA1 gene, indicating that BRCA1 dysfunction is a serious threat to typical cell procedures¹⁷. Furthermore, BRCA1 mutated tumor cells have an increased likelihood of being estrogen receptor negative, progesterone receptor negative, and less likely to overexpress the Human Epithelial Growth Factor 2 (HER2). This type of Triple Negative Breast Cancer (TNBC) causes the cancer to be more aggressive and have a higher histologic grade than spontaneous cancer cells³¹.

Double Strand Breaks in Cancer Therapy

It is thought that chemotherapies attack cancer cells by delivering DSBs that they fail to repair³³. DNA damage-associated therapies include Radiotherapy and Ionizing Radiation, Cytotoxic Chemotherapy, and DDR Modulators³².

However, many of these therapies cause multiple different types of DNA damage, not just DSBs, or they do not directly cut DNA, but rather indirectly lead to DSB formation, such as by inhibiting protein-DNA dissociation. For example, etoposide is a drug that inhibits dissociation of topoisomerase II from DNA, causing DSBs³³.

Inducing DSBs via CRISPR-Cas9

Another way to induce DSBs is through CRISPR-Cas9 techniques. Doench et al. (2014, 2016) have designed guide RNAs with a high efficacy, low off-target risk. These guide RNAs are designed differently than their average counterparts due to their target being upstream of an NGG PAM sequence. These “high affinity” sgRNAs were able to cleave at the target site, and thus alleles were able to be nullified with CRISPR-Cas9 when targeted with a guide RNA corresponding to their sequence^{34,35}. Van den Berg et al. (2018) further validates the use of these sgRNAs to target specific sequences in the genome of RPE1 cells, as used in this project, using sequence-specific guides to direct Cas9 cleavage (Figure 3)³⁶.

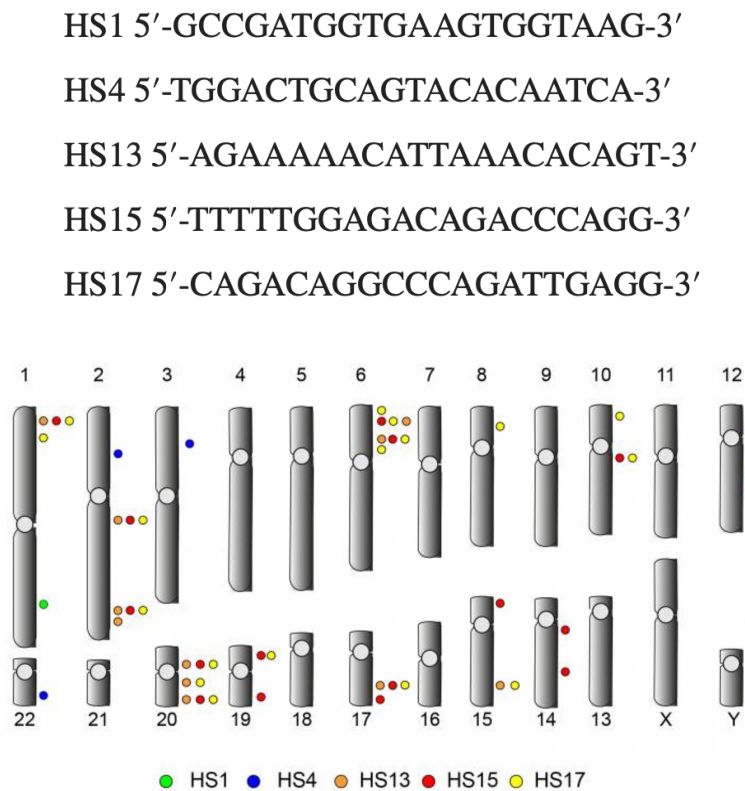


Figure 3: Van den Berg et al. (2018) show the sequences and locations of sgRNAs to induce targeted DSBs. The sequence of the sgRNA (above) guides the Cas9 endonuclease to sites in the genome, causing an amount of cuts corresponding to that sequence.

Project Introduction

While DSBs and the mechanisms of DSB repair are understood, there is an opportunity to better understand the cellular response for Double Strand Breaks and avoid the complexity of chemotherapy-induced DSBs. In addition, there is an opportunity to better understand the timeline of this apoptotic response through the nuclear morphology in the days following DSB induction. This project explores the relationship between DSBs, cell death, and apoptosis through measuring caspase-3/7 activity and nuclear abnormality ratios. 0, 13, or 100 Double Strand Breaks were induced using CRISPR transfection, with etoposide as a positive control. After DSBs were confirmed with a γ H2AX assay, the first phase of the project was to perform cleaved caspase-3/7 fluorescent assays 48 hours after DSB induction. To better understand the timeline of the apoptosis response after DSBs, the next phase of the project determined the ratios of nuclear abnormalities to total nuclei 24, 48, and 72 hours after DSB induction. To explore the influence of BRCA 1 on nuclear morphology of apoptosis, control RPE cells were compared with BRCA1 Knock-Out (B1KO) cell lines (Figure 4).

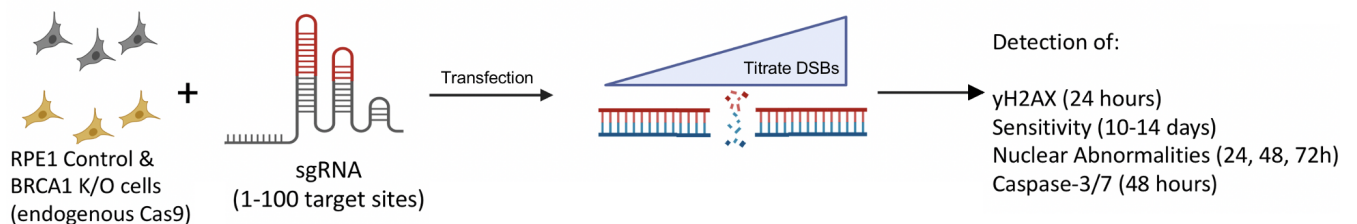


Figure 4: Schematic of Project Approach. RPE cells with endogenous Cas9 are transfected with certain guide RNAs to induce DSBs. Then, cell response is measured using γ H2AX, Sensitivity, Nuclear Abnormality, and Caspase-3/7 Assays.

Methods

Cell Lines

The BRCA-1 Knockout (B1KO) and Wild Type (WT) Retinal Pigment Epithelium (RPE) cell lines used in this experiment were integrated with Cas9, courtesy of the D. Durocher Lab (Lunenfeld-Tanenbaum Research Institute). Cells were cultured in an incubator at 37 degrees Celsius and maintained using Dulbecco's Modified Eagle Medium (DMEM) (Thermo Fisher Catalog #11965084) supplemented with 10% Fetal Bovine Serum (FBS) and 1% Penicillin-Streptomycin. Cells were cultured in 150mm plates (Corning Catalog #430599).

Cell Seeding

Cells were seeded for experiments in 6-well plates (Corning Catalog #3516). 200,000 cells were seeded for each DSB scenario/controls using a hemocytometer. During cell seeding, cells were maintained in Dulbecco's Modified Eagle Medium (DMEM) (Thermo Fisher Catalog #11965084) supplemented with 10% Fetal Bovine Serum (FBS).

Induction of Double Strand Breaks, and Control Scenarios

For the all cellular response assays used in this project, DSBs were induced. Due to the endogenous Cas9 endonuclease in the cell lines used, DSBs were induced using CRISPR. For each DSB condition, 250 uL of the transfection system was added to the cell sample after 2 mL of DMEM supplemented with 10% FBS was added. The transfection system was prepared with 2.87% vol. RNAiMax Lipofectamine Transfection Buffer, 1.59% vol. guide RNA in OPTI-MEM (Thermo Fisher Catalog #31985070). Guide RNAs were ordered through IDT (Alt-R CRISPR-Cas9 sgRNA). sgRNAs targeting 4,13,15, and 17 sites were described in van de Berg et al.,

(2018). sgRNAs targeting 1 site (AAVS1) and 100 sites (CAG) were generated by the Brodsky Lab (UMass Chan Medical School, MCCB). Sequences are as follows:

AAVS1: 5-GTCCCCTCCACCCCACAGTG-3

HS4: 5-TGGACTGCAGTACACAATCA-3

HS13: 5-AGAAAAACATTAACACAGT-3

HS15: 5-TTTTTGGAGACAGACCCAGG-3

HS17: 5-CAGACAGGCCAGATTGAGG-3

CAG: 5-AGCAGCAGCAGCAGCAGCAGCAG-3

Non-targeting: 5- GTAGCGAACGTGTCCGGCGT-3

The zero DSBs condition acted as a negative control for the experiment. In that scenario, OPTI-MEM was combined with the Lipofectamine RNAiMax reagent, but no guide RNA was added. As a positive control for apoptosis during the Caspase-3/7 experiments, cells were treated with 50 uM etoposide and covered in tinfoil.

yH2AX Foci Assay

To confirm the induction of DSBs with Crispr-Cas9, a yH2AX foci assay was performed in technical triplicate. This immunofluorescent assay identifies phosphorylated H2AX, a histone variant of the H2A protein. Following cell permeabilization with PBS+0.5% Triton-X and fixation with 4% Paraformaldehyde (PFA) in PBS, cells were incubated for 1 hour with a 1:500 dilution in 3% BSA of Millipore JBW301 (anti-phospho-histone) yH2AX primary antibody. Then, samples were treated with a 1:250 dilution of Invitrogen Alexaflour 488 anti-mouse secondary antibody and covered in tinfoil for 1 hour. After staining nuclei with a 1:500 dilution in PBS of Hoechst for 30 minutes, cells were mounted to coverslips. Samples were imaged with fluorescent microscopy using ZEISS Imaging software, at 200x total magnification, with exposures of eGFP 175.00 ms, DAPI 25.00 ms.

To analyze the γ H2AX signal in these images, a nuclear range for each scenario was determined via FIJI software's linear measuring tool (ImageJ Version 2.9.0). Data from these images was gathered using CellProfiler software (Broad Institute Version 4.2.1), where the mean intensity of eGFP signal was measured for each nuclei imaged. Graphs were made using GraphPad Prism (Dotmatics version 9.1.2).

Cell Survival

After 10-14 days of cell colony growth in a 6-well plate with complete media, methanol/0.5% Crystal Violet (0.5g Crystal Violet, 27 mL 37% Formaldehyde, 100 mL 10x PBS, 10 mL methanol, 863 deionized water to 1L) was used to stain surviving cell colonies. After incubation, plates were washed with water. Cell colonies were counted manually, and survival was normalized to the control that did not have sgRNA added, but was otherwise treated with the same buffers and conditions.

Cleaved Caspase 3/7 Assay

To measure the intensity of apoptosis after DSB induction, a Caspase-3/7 was performed 48 hours after transfection. Invitrogen's CellEvent™ Caspase-3/7 Detection Reagent (GDR) (Thermo Fisher Catalog #10423) was used to measure the intensity of apoptosis. Cells were treated with 2 mL of 3.33 μ M of GDR in 5% FBS in PBS under dark conditions. After covering for a 30 minute incubation in 37 deg. C, cells were fixed with 4% PFA in PBS and stained with a 1:500 dilution in PBS of Hoechst for 15 minutes. Samples were then mounted to slides and imaged using fluorescent microscopy using ZEISS Imaging software, at 630x total magnification with oil, with exposures of eGFP 70.00 ms, DAPI 14.00 ms. This experiment was performed in technical triplicate.

To analyze the intensity of apoptosis in these images, a nuclear range for each scenario was determined via FIJI software's linear measuring tool (ImageJ Version 2.9.0). Data from these images was gathered using CellProfiler software (Broad Institute Version 4.2.1), where the average intensity of eGFP signal was measured for each nuclei imaged. Graphs were made using GraphPad Prism (Dotmatics version 9.1.2).

Nuclear Abnormalities

To record the number of nuclear abnormalities occurring in a sample, nuclei were counted using FIJI ImageJ's cell counter software. Images taken at 20x were blindly relabeled. The number of nuclei stained with DAPI were calculated. Nuclear abnormalities were then counted, and the percentage of abnormalities were calculated. The average percentage of abnormalities were calculated for each circumstance of DSB and days since induction of those DSBs. This experiment was performed in technical replicate.

DNA-PK Immunofluorescence

Cells were seeded onto coverslips in 6-well plates. Cells were put on ice for 1 minute then pre-extracted with ice cold PBS+0.25% Triton on ice for 1 minute and washed with PBS. Cells were then fixed with 4% paraformaldehyde in PBS for 15 minutes. Cells were pre-extracted again with ice cold PBS+0.5% Triton on ice for 1 minute and washed with PBS. 3% BSA in PBS blocking solution was added for 30 minutes at room temperature. Cells were washed twice with PBS-T (0.01% Tween) and incubated with primary antibody (DNA-PK Abcam ab18192 1:200 dilution in PBS+3% BSA) for 1 hour at room temperature. After three PBS-T washes cells were incubated with a secondary antibody, Alexa fluor 488 (ThermoFisher Catalog #A32731) in 1:250 dilution in PBS+3% BSA) for 1 hour at room temperature. After three PBS-T washes, cells were

incubated with Hoechst stain (ThermoFisher Catalog #62249) as a 1:500 dilution in PBS for 30 minutes at room temperature. After two PBS washes, coverslips were mounted with Prolong (Invitrogen Catalog #P36930). Images were collected by fluorescent microscopy (Axioplan 2 Imaging and Axio Observer, Zeiss) at a constant exposure time in each experiment. Number of foci or mean intensity of immunofluorescence for each nucleus were measured with Cell Profiler software from the Broad Institute.

Results

Double Strand Breaks can be made with CRISPR

To confirm the induction of DSBs, a γ H2AX foci assay was performed. The γ H2AX assay identifies the ends of DSBs by tagging the γ H2AX protein (a key step in the cell's DSB recognition) with a fluorescent antibody. The average fluorescence from each nuclei analyzed is plotted. Results from this assay show a statistically significant increase ($p < 0.001$) in γ H2AX foci with titrating DSBs (Figure 5). These results suggest that DSBs are in fact being induced through CRISPR techniques.

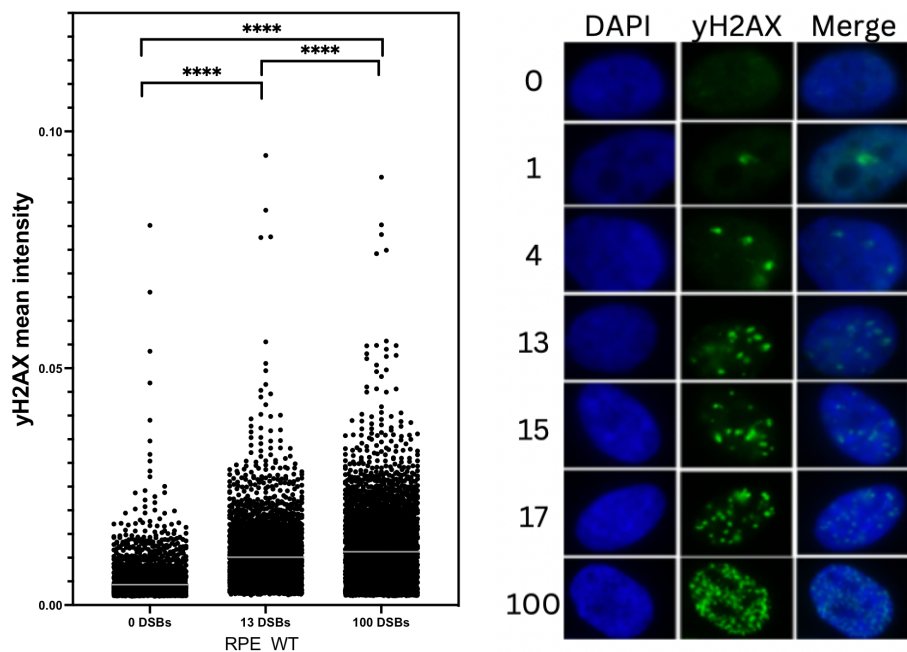


Figure 5: γ H2AX foci assay of increasing DSBs in RPE cells (left) and sample images of γ H2AX foci (right), 630x with oil. A statistically significant increase is shown in the γ H2AX average signal as the number of induced DSBs increase.

CRISPR DSBs are cell lethal

The next phase of the project determines whether or not cells were being killed by DSBs. A cell survival assay was used to determine the percent survival of RPE cells with increasing DSBs induced by CRISPR. By plotting the percent survival of colonies, it was determined that cell death was correlated to the number of DSBs induced (Figure 6).

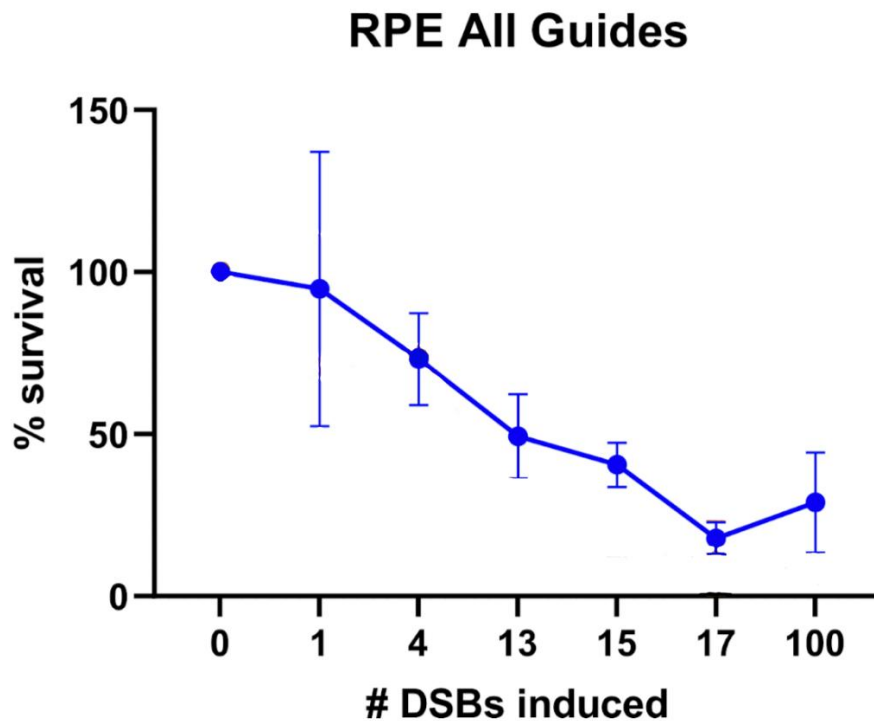


Figure 6: Survival assay of RPE cells after DSBs were induced. Guide RNA corresponding to 1, 4, 13, 15, 17, and 100 DSBs was utilized to explore the nature of various amounts of DSBs. By plotting the percent survival of colonies, it was determined that cell death was correlated to the number of DSBs induced.

DSBs can cause cell killing by Apoptosis

Caspase-3/7 Assay

While the amount of cell death was determined in the cell survival assays, the cause of cell death was not confirmed. An assay measuring caspase-3/7 activity was performed to explore whether these cells were dying through the apoptotic pathway. The assay was run 48 hours after DSBs or the positive control, etoposide, were induced. Results from this assay also show a significantly

increasing average signal for apoptosis as the number of DSBs increase (Figure 7). While the contrast between apoptotic signals for the 0 DSB control and the DSBs/etoposide is consistently significant, the similar signals for 13, 100, and etoposide results suggest that there could be a limit to the apoptosis signal induced by DSBs.

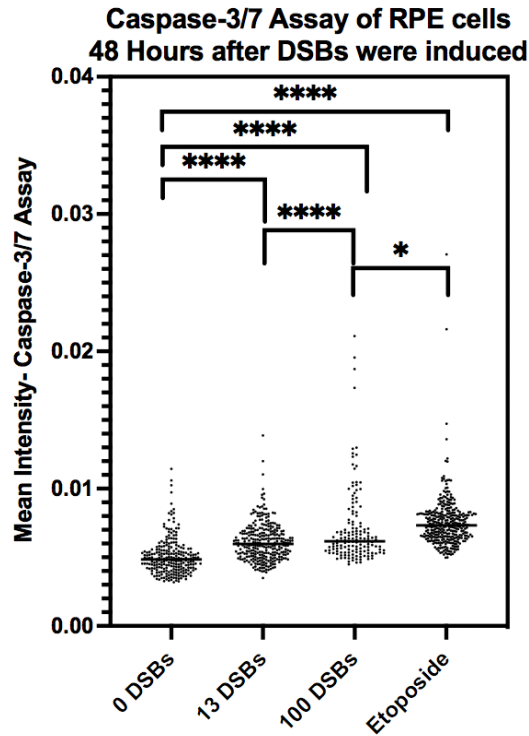


Figure 7: Average Intensity of Apoptotic Signal via Caspase-3/7 Assay. A significant increase in apoptotic levels was seen compared to the 0 DSB control, showing apoptotic activity.

Nuclear Abnormalities

To further explore the timeline of apoptosis in these scenarios, nuclear abnormality assays were used to measure the ratio of nuclear abnormalities. These assays were performed 24, 48, and 72 hours after DSB/etoposide induction to better explore the timeline of apoptosis in these scenarios, rather than only 48 hours as done with the Caspase-3/7 assay. These results quantified the nuclear phenotypes associated with apoptosis as a ratio to total nuclei (Figure 9). Results

showed a stepwise increase with each 24 hour period for the DSBs induced, with 100 DSB scenarios causing the most nuclear abnormalities. By 72 hours, 100 DSBs caused abnormalities for nearly 1 in 5 nuclei. 0 DSBs were a reliable negative control, showing very few abnormalities. Interestingly, the etoposide positive control did not show a stepwise increase of abnormality percentage, instead having a relatively low percentage (4-5%) over the first two days analyzed, and increasing to 14% by the third day.

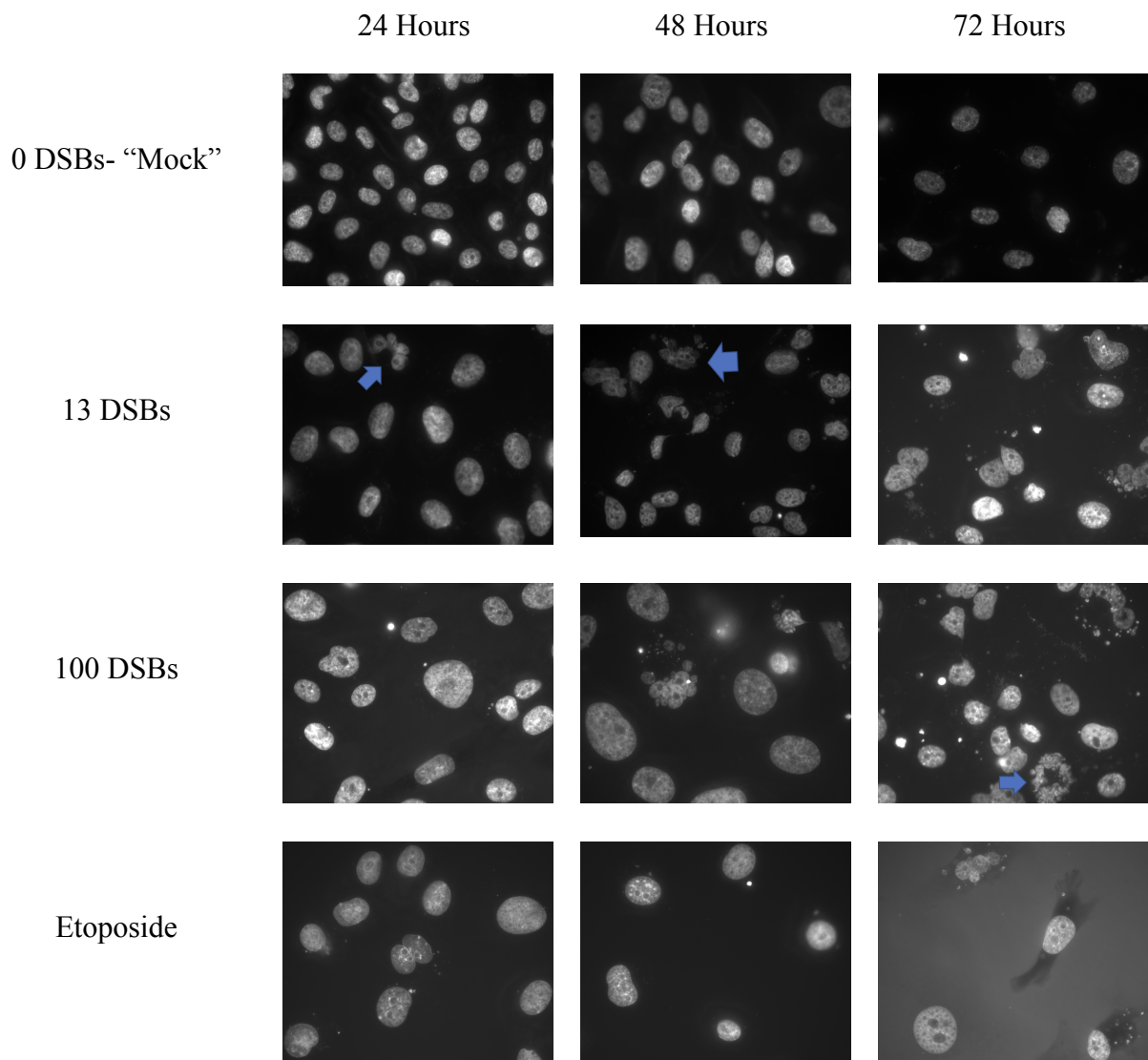


Figure 8: Sample Images of Nuclei Under Each DSB Scenario, 630x with oil. To demonstrate, some abnormalities are denoted with arrows, though more abnormalities are observed in these images.

Nuclear Abnormalities per DSBs, RPE Cells

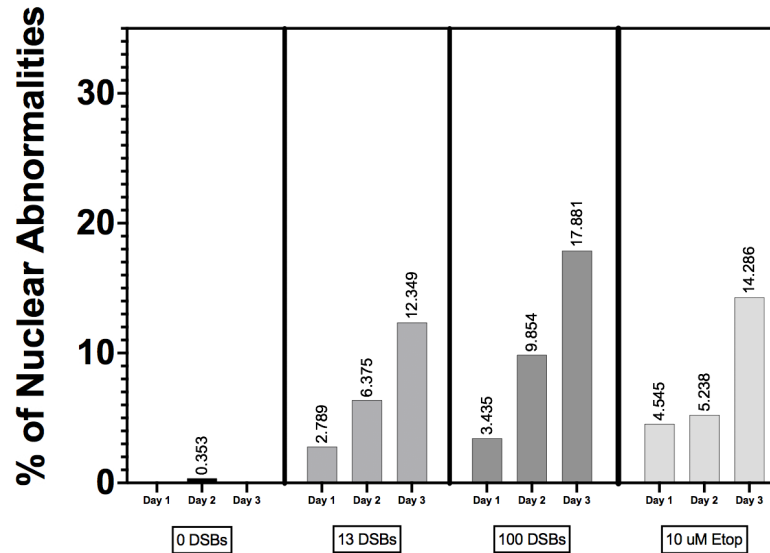


Figure 9: Nuclear Abnormalities in RPE cells at 24, 48, and 72 Hours. In a blind nuclear abnormality assay, nuclei were imaged at 200x then quantified. Nuclear abnormalities were quantified to increase with time, and the presence of abnormalities was quantified to be slightly higher with more DSBs.

Exploring Mechanisms of DSB Repair

To test whether Double Strand Breaks are repaired by a particular pathway, a BRCA1 deficient cell line was used to target homologous recombination. The survival, apoptotic, and nuclear abnormality assays were performed again with the Durocher BRCA 1 knockout RPE cell lines (Figure 10). For further exploration, survival assays were determined for BRCA 1 Knockout cell lines. For the Survival Assays, B1KO lines showed more sensitivity to DSBs, but were not vastly more sensitive compared to control lines. For the apoptotic measurements, the caspase-3/7 assay for BRCA-1 yielded an inconclusive caspase-3/7 result - there was variability across experiment replicates. Nuclear abnormality levels were consistent with control lines for 0, 100, and etoposide scenarios; 13 DSBs showed a nearly two-fold measure of nuclear abnormalities.

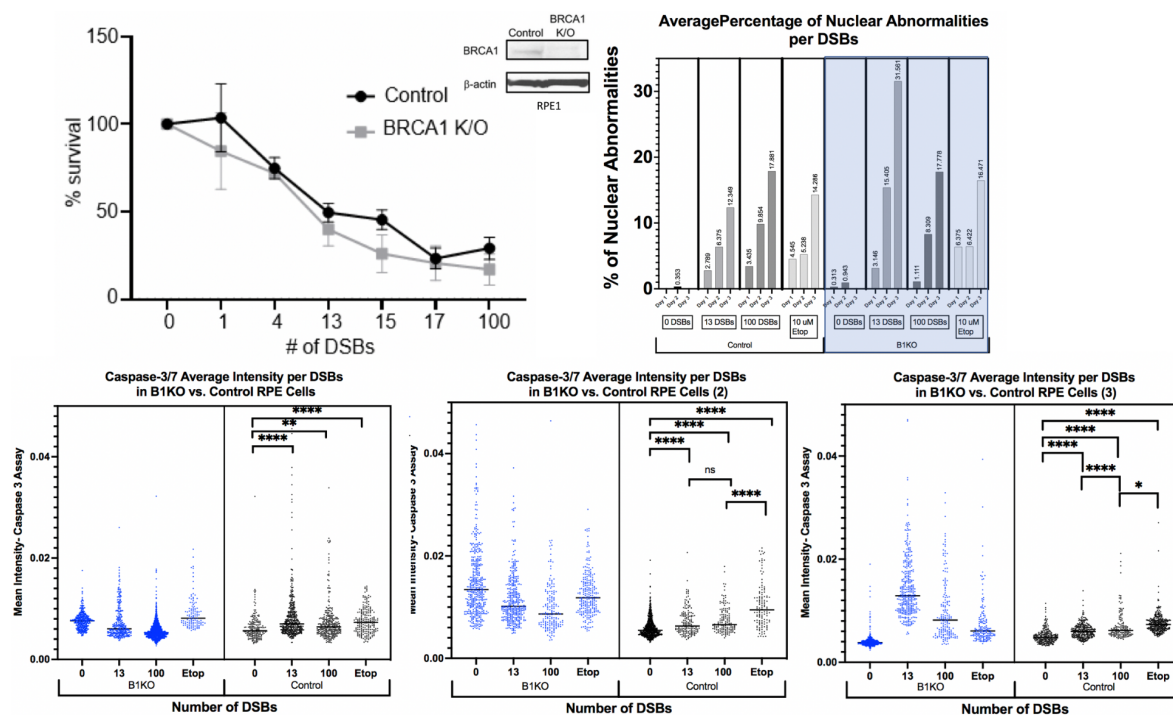


Figure 10: Comparison of BRCA1 Knockout cell lines vs. Control for Survival Assay, Nuclear Abnormality Assay, and Caspase-3/7 Assay. For the Survival Assays, B1KO lines showed more sensitivity to DSBs, but were not vastly more sensitive compared to control lines. For the apoptotic measurements, The caspase-3/7 assay for BRCA-1 yielded an inconclusive caspase-3/7 result - there was variability across experiment replicates. Nuclear abnormality levels were consistent with control lines for 0, 100, and etoposide scenarios; 13 DSBs showed a nearly two-fold measure of nuclear abnormalities.

To explore whether the DSBs were being repaired through Non-Homologous End Joining, a DNA-PK assay was used to quantify the amount of DNA-PK, a central protein in the NHEJ pathway. Results showed that DNA-PK levels correlate with the number of DSBs induced. Additionally, B1KO cells of the same line had higher levels of DNA-PK than their control counterpart. When blocking NHEJ with a DNA-PK inhibitor, survival of Control cells became nearly extinct with only 4 DSBs, confirming that cells turn to NHEJ for the majority of DSB repair (Figure 11).

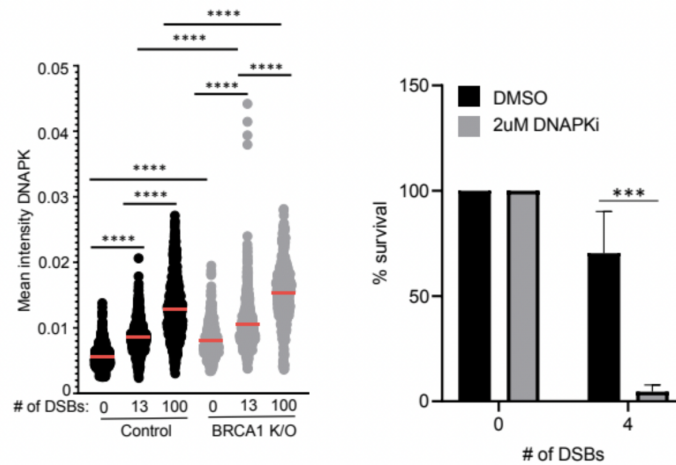


Figure 11: Exploring NHEJ as DSB Repair. A DNA-PK average intensity signal (left) showed significant increase of DNA-PK levels with increasing DSBs. B1KO cell lines showed higher DNA-PK signal than Control, indicating a more active NHEJ pathway. Additionally, inhibiting the NHEJ pathway in B1KO cell lines with 2 uM DNA-PKi causes low survival rates after inducing just 4 DSBs.

Discussion

Project Discussion

The experiments performed throughout this project sought to better understand the relationship between the number of DSBs, cell death, apoptosis, and the pathways at work during DSB repair. Additionally, it explored the effectiveness of CRISPR in causing cell responses associated in DSBs. Though cytotoxic and radiation chemotherapies have been extensively studied, this project focuses on one aspect of the therapeutic mechanisms, DSBs, and aims to quantify its effects.

Due to the validity of the γ H2AX assay and adherence to assay protocols, the results seen throughout the project can be attributed to the effects of DSB induction. It is determined that the impact of DSBs on cell death, apoptosis, and nuclear abnormalities was titratable in the conditions tested. One area of challenge involved the Caspase-3/7 assay. Assay optimization was reached when reagents for the assay were added in a different order than instructed (FBS added after the GDR reagent) to optimize diffusion of the fluorescent marker through the solution.

However, the results of the B1KO cell line Caspase-3/7 assay were inconclusive as results were inconsistent across replicates. As the control was reproducible, the B1KO results could be due to either inconsistency with cell response, or more likely, an interference of the assay signal- some B1KO samples had high backgrounds under the fluorescent microscope, which could distort the signal measured. Using a different assay with another biomarker to measure apoptosis levels would be helpful in confirming whether apoptosis pathways are readily occurring in B1KO cell lines. This was attempted with the Nuclear Morphology assays, but a more objective biomarker measurement would be better when drawing conclusions about “BRCAness” and apoptosis. The Nuclear Morphology assay was an interesting way to measure

cell effects and observe the cellular response. In the blind quantification, very reproducible results were seen between replicates. Stepwise increases in abnormality percentage indicate that more cells are experiencing apoptosis as time continues. The high percentage of nuclear abnormalities for 13 DSB B1KO conditions pose an area of inquiry. Cell survival assays do not see a large disparity between control and B1KO lines for 13 DSB survival, yet these nuclear abnormality levels are nearly twice as high in B1KO than control lines. Further experimentation, and a reliable biomarker for apoptosis in B1KO lines, could explore reasons for this occurrence and determine if there is a threshold for the cell's ability to repair DSBs.

Future Directions

Future directions of the project would include further exploring the effect of fewer DSBs on Apoptosis and nuclear morphology. As the amount of DSBs and cell survival seem to be inversely correlated, exploration of the cellular response of fewer DSBs, such as 1 or 4, could provide more insight about where the cellular threshold is for repair. How many DSBs does it take to cause the apoptotic response?

Additionally, further investigation regarding the time to cell death, instead of just apoptosis, could indicate whether the time to death is altered with a DSB. Understanding DSB-induced cell death with BRCA1 deficient cells could provide a better understanding of DSB sensitivity in cancer cells. Performing these experiments with cancer cell lines, rather than the RPE B1KO model cell line, could also explore cancer cells' sensitivity to DSBs.

MDA-MB436, for example, is a line of breast cancer cells with a mutated BRCA1 gene³⁹. Using this line could investigate how cancer cells respond to DSBs, and their mechanisms of DNA repair in light of BRCA1 dysfunction.

The cell cycle plays a role in which repair pathway is used, G1-phase NHEJ, or S/G2-phase HR. The cells analyzed were not cell cycle synchronized, and that may impact cell response to DSBs. Further exploration into cells with synchronized cell cycles could provide more information about these effects.

Implications for Cancer Therapy

BRCA 1 is a known tumor suppressor gene, and the BRCA1 protein is involved in many processes, including the higher fidelity HR for DSB repair. However, in survival assays, there is not a stark differentiation in cell death between BRCA1 deficient and proficient cells after DSB induction (Figure 6).

When BRCA1 is deficient, the cell utilizes other pathways to compensate. Treating BRCA1 deficient cells with PARP inhibitors, for example, is a way to target single strand annealing pathways, another backup process in DSB repair. If BRCA1 is no longer functional, inhibiting backup pathways used in DSB repair is a known possibility for inducing death in those cells. This has implications on the next generations of cancer treatment, as researchers set out to find advancements in cancer therapy, specifically as the demand for therapies that target cancer efficiently but minimize harm to other cells in the body.

For BRCA1- related cancers, seeking where BRCA1-related pathways have alternate pathways that are easily inhibited could unlock the key to target cancer cells only. For example, ssDNA gaps have been shown to exhibit more hypersensitivity than DSB induction and underlie cytotoxicity³⁷.

Another challenge in anticancer research lies in cancer cell's deregulation or evasion of apoptosis. BRCA 1 deficient cells have been known to resist apoptosis, utilizing signals such as cAMP to prevent p53-dependent apoptosis in BRCA1 deficient ovarian cells³⁸. Determining

ways to overcome this apoptotic resistance could provide a breakthrough in causing cancer cell death.

In conclusion, this project aimed to explore the effects of DSBs on apoptotic cell response. As this is a select component of the relationship between DNA damage and cell response mechanisms, a better understanding of different DNA lesions' effects could be the key to exploiting cancer cell vulnerability in drug therapy.

Bibliography

1. Cannan, W. J., & Pederson, D. S. (2016). Mechanisms and consequences of Double-Strand DNA break formation in chromatin. *Journal of Cellular Physiology*; 231(1), 3–14. <https://doi.org/10.1002/jcp.25048>
2. Chapman JR, Taylor MR, Boulton SJ (2012) Playing the end game: DNA double-strand break repair pathway choice. *Mol Cell*;47(4):497-510. <https://10.1016/j.molcel.2012.07.029>.
3. Khanna, K. K., & Jackson, S. P. (2001). DNA double-strand breaks: signaling, repair and the cancer connection. *Nature Genetics*, 27(3), 247–254. <https://doi.org/10.1038/85798>
4. Jackson, S. P. (2002). Sensing and repairing DNA double-strand breaks. *Carcinogenesis*, 23(5), 687–696. <https://doi.org/10.1093/carcin/23.5.687>
5. Rickman, K., & Smogorzewska, A. (2019). Advances in understanding DNA processing and protection at stalled replication forks. *The Journal of Cell Biology*, 218(4), 1096–1107. <https://doi.org/10.1083/jcb.201809012>
6. Sabatinos, S.A. (2010) Recovering a stalled replication fork. *Nature Education*. <https://www.nature.com/scitable/topicpage/recovering-a-stalled-replication-fork-14436634/>
7. Zeman, M. K., & Cimprich, K. A. (2014). Causes and consequences of replication stress. *Nature Cell Biology*, 16(1), 2–9. <https://doi.org/10.1038/ncb2897>
8. Shen, Z. (2011). Genomic instability and cancer: An introduction. *Journal of Molecular Cell Biology*, 3(1), 1–3. <https://doi.org/10.1093/jmcb/mjq057>
9. Wei Dai, Y. Y. (2014). Genomic instability and cancer. *Journal of Carcinogenesis & Mutagenesis*, 05(02). <https://doi.org/10.4172/2157-2518.1000165>
10. Mills, K.D., Ferguson, D.O. and Alt, F.W. (2003), The role of DNA breaks in genomic instability and tumorigenesis. *Immunological Reviews*, 194: 77-95. <https://doi.org/10.1034/j.1600-065X.2003.00060.x>
11. Krejci, L., Altmannova, V., Spirek, M., & Zhao, X. (2012). Homologous recombination and its regulation. *Nucleic Acids Research*, 40(13), 5795–5818. <https://doi.org/10.1093/nar/gks270>
12. Mehta, A., & Haber, J. E. (2014). Sources of DNA Double-Strand breaks and models of recombinational DNA repair. *Cold Spring Harbor Perspectives in Biology*, 6(9), a016428–a016428. <https://doi.org/10.1101/cshperspect.a016428>
13. Davis, A. J., & Chen, D. J. (2013). DNA double strand break repair via non-homologous end-joining. *Translational Cancer Research*, 2(3), 130–143. <https://doi.org/10.3978/j.issn.2218-676X.2013.04.02>
14. Podhorecka, M., Skladanowski, A., & Bozko, P. (2010). H2AX Phosphorylation: Its role in DNA damage response and cancer therapy. *Journal of Nucleic Acids*, 2010, 920161. <https://doi.org/10.4061/2010/920161>

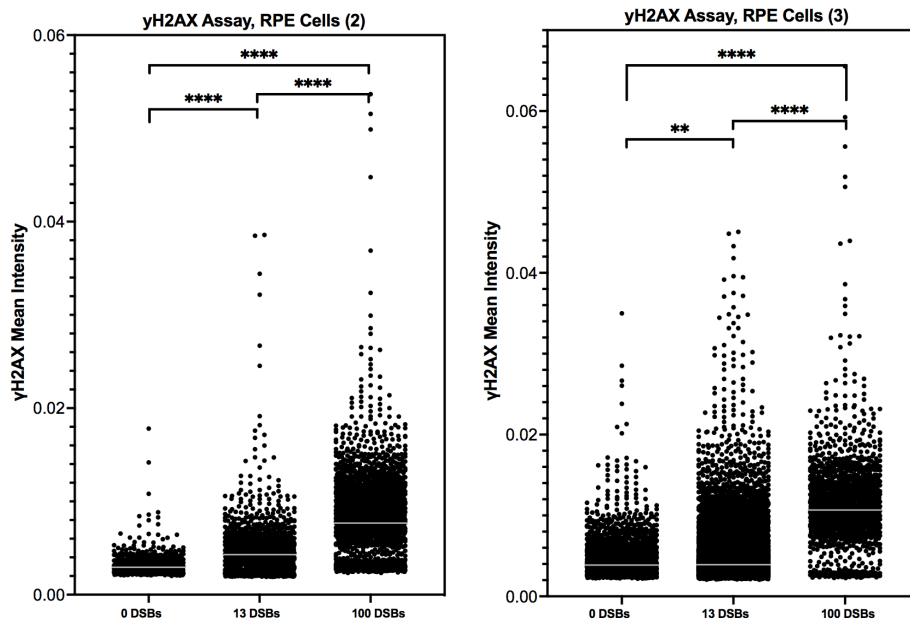
15. Kuo, L. J., & Yang, L. X. (2008). Gamma-H2AX - a novel biomarker for DNA double-strand breaks. *In vivo (Athens, Greece)*, 22(3), 305–309.
16. Ivashkevich, A., Redon, C. E., Nakamura, A. J., Martin, R. F., & Martin, O. A. (2012). Use of the γ -H2AX assay to monitor DNA damage and repair in translational cancer research. *Cancer Letters*, 327(1-2), 123–133. <https://doi.org/10.1016/j.canlet.2011.12.025>
17. National Library of Medicine (2023) BRCA1 DNA Repair Associated Gene. *National Institute of Health*. <https://www.ncbi.nlm.nih.gov/gene/672>
18. Clark, S. L., Rodriguez, A. M., Snyder, R. R., Hankins, G. D., & Boehning, D. (2012). Structure-Function Of The Tumor Suppressor BRCA1. *Computational and Structural Biotechnology Journal*, 1(1), e201204005. <https://doi.org/10.5936/csbj.201204005>
19. Roy, R., Chun, J., & Powell, S. N. (2011). BRCA1 and BRCA2: different roles in a common pathway of genome protection. *Nature reviews. Cancer*, 12(1), 68–78. <https://doi.org/10.1038/nrc3181>
20. Takaoka, M., & Miki, Y. (2018). BRCA1 gene: function and deficiency. *International Journal of Clinical Oncology*, 23(1), 36–44. <https://doi.org/10.1007/s10147-017-1182-2>
21. Elmore, S. (2007). Apoptosis: a Review of Programmed Cell Death. *Toxicologic Pathology*, 35(4), 495–516. <https://doi.org/10.1080/01926230701320337>
22. Mcllwain, D. R., Berger, T., & Mak, T. W. (2013). Caspase functions in cell death and disease. *Cold Spring Harbor Perspectives in Biology*, 5(4), a008656. <https://doi.org/10.1101/cshperspect.a008656>
23. Wolf, B. B., Schuler, M., Echeverri, F., & Green, D. R. (1999). Caspase-3 Is the Primary Activator of Apoptotic DNA Fragmentation via DNA Fragmentation Factor-45/Inhibitor of Caspase-activated DNase Inactivation. *Journal of Biological Chemistry*, 274(43), 30651–30656. <https://doi.org/10.1074/jbc.274.43.30651>
24. Porter, A. G., & Jänicke, R. U. (1999). Emerging roles of caspase-3 in apoptosis. *Cell Death and Differentiation*, 6(2), 99–104. <https://doi.org/10.1038/sj.cdd.4400476>
25. Tyas, L., Brophy, V. A., Pope, A., Rivett, A. J., & Tavaré, J. M. (2000). Rapid caspase-3 activation during apoptosis revealed using fluorescence-resonance energy transfer. *EMBO Reports*, 1(3), 266–270. <https://doi.org/10.1093/embo-reports/kvd050>
26. Brentnall, M., Rodriguez-Menocal, L., De Guevara, R. L., Cepero, E., & Boise, L. H. (2013). Caspase-9, caspase-3 and caspase-7 have distinct roles during intrinsic apoptosis. *BMC Cell Biology*, 14, 32. <https://doi.org/10.1186/1471-2121-14-32>
27. Fischer, EG. (2020) Nuclear Morphology and the Biology of Cancer Cells. *Acta Cytologica*; 64:511–519. <https://doi.org/10.1159/000508780>
28. Eidet, J. R., Pasovic, L., Maria, R., Jackson, C. J., & Utheim, T. P. (2014). Objective assessment of changes in nuclear morphology and cell distribution following induction of apoptosis. *Diagnostic Pathology*, 9, 92. <https://doi.org/10.1186/1746-1596-9-92>
29. Hollville, E. and Martin, S.J. (2016) Measuring apoptosis by microscopy and flow cytometry. *Curr. Protoc. Immunol.* 112: 14.38.1- 14.38.24. <https://doi.org/10.1002/0471142735.im1438s112>

30. Barros, L. F., Kanaseki, T., Sabirov, R., Morishima, S., Castro, J., Bittner, C. X., Maeno, E., Ando-Akatsuka, Y., & Okada, Y. (2003). Apoptotic and necrotic blebs in epithelial cells display similar neck diameters but different kinase dependency. *Cell Death & Differentiation*, 10(6), 687–697. <https://doi.org/10.1038/sj.cdd.4401236>
31. Petrucelli, N., Daly, M. B., & Tuya Pal. (2016, December 15). *BRCA1- and BRCA2-Associated Hereditary Breast and Ovarian Cancer*. National Institute of Health; University of Washington, Seattle. <https://www.ncbi.nlm.nih.gov/books/NBK1247/>
32. Reuvers, T. G. A., Kanaar, R., & Nonnekens, J. (2020). DNA Damage-Inducing Anticancer Therapies: From Global to Precision Damage. *Cancers*, 12(8), 2098. <https://doi.org/10.3390/cancers12082098>
33. Li, L. Y., Guan, Y. D., Chen, X. S., Yang, J. M., & Cheng, Y. (2021). DNA Repair Pathways in Cancer Therapy and Resistance. *Frontiers in Pharmacology*, 11, 629266. <https://doi.org/10.3389/fphar.2020.629266>
34. Doench, J. G., Hartenian, E., Graham, D. B., Tothova, Z., Hegde, M., Smith, I., ... Root, D. E. (2014). Rational design of highly active sgRNAs for CRISPR-Cas9-mediated gene inactivation. *Nature Biotechnology*, 32(12), 1262–1267. <https://doi.org/10.1038/nbt.3026>
35. Doench, J. G., Fusi, N., Sullender, M., Hegde, M., Vaimberg, E. W., Donovan, K. F., ... Root, D. E. (2016). Optimized sgRNA design to maximize activity and minimize off-target effects of CRISPR-Cas9. *Nature Biotechnology*, 34(2), 184–191. <https://doi.org/10.1038/nbt.3437>
36. van den Berg, J., G Manjón, A., Kielbassa, K., Feringa, F. M., Freire, R., & Medema, R. H. (2018). A limited number of double-strand DNA breaks is sufficient to delay cell cycle progression. *Nucleic acids research*, 46(19), 10132–10144. <https://doi.org/10.1093/nar/gky786>
37. Panzarino, N. J., Krais, J. J., Cong, K., Peng, M., Mosqueda, M., Nayak, S. U., Bond, S. M., Calvo, J. A., Doshi, M. B., Bere, M., Ou, J., Deng, B., Zhu, L. J., Johnson, N., & Cantor, S. B. (2021). Replication Gaps Underlie BRCA Deficiency and Therapy Response. *Cancer Research*, 81(5), 1388–1397. <https://doi.org/10.1158/0008-5472.CAN-20-1602>
38. Yue, W., Ma, J., Xiao, Y., Wang, P., Gu, X., Xie, B., & Li, M. (2022). The Apoptotic Resistance of BRCA1-Deficient Ovarian Cancer Cells is Mediated by cAMP. *Frontiers in Cell and Developmental Biology*, 10. <https://doi.org/10.3389/fcell.2022.889656>
39. Dai, X., Cheng, H., Bai, Z., & Li, J. (2017). Breast Cancer Cell Line Classification and Its Relevance with Breast Tumor Subtyping. *Journal of Cancer*, 8(16), 3131–3141. <https://doi.org/10.7150/jca.18457>

Supplementary Figures

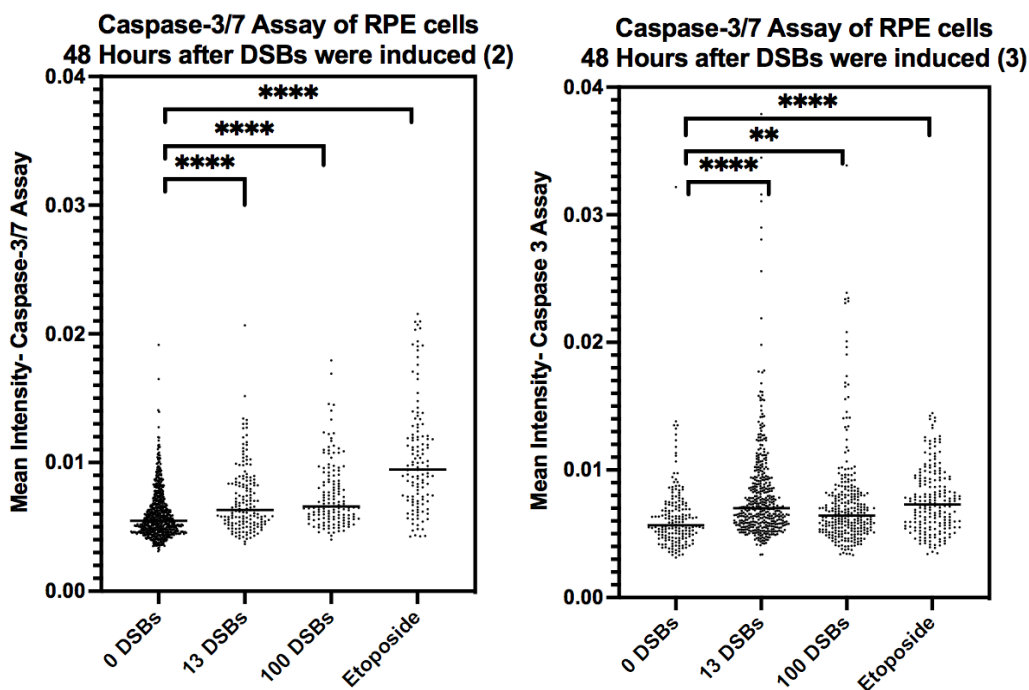
Supplementary Figures 1: γ H2AX Triplicate Results

These figures include the additional results of the γ H2AX assays. Results from this assay show a statistically significant increase ($p < 0.001$) in γ H2AX foci with titrating DSBs. These results suggest that DSBs are in fact being induced through CRISPR techniques.



Supplementary Figures 2: Caspase-3/7 Assay Triplicate Results

These figures contain the remaining data gathered when performing the Caspase-3/7 apoptotic assays. Results from this assay also show a significantly increasing average signal for apoptosis as the number of DSBs increase. While the contrast between apoptotic signals for the 0 DSB control and the DSBs/etoposide is consistently significant, the similar signals for 13, 100, and etoposide results suggest that there could be a limit to the apoptosis signal induced by DSBs.



Supplementary Figure 3: Nuclear Abnormalities Replicate

This figure includes the second replicate of the nuclear abnormalities assay. Nuclear Abnormalities were quantified in RPE cells at 24, 48, and 72 Hours after DSB induction. In a blind nuclear abnormality assay, nuclei were imaged at 200x then quantified. Nuclear abnormalities were quantified to increase with time, and the presence of abnormalities was quantified to be slightly higher with more DSBs.

Nuclear Abnormalities per DSBs, RPE Cells

